Growth of epitaxial iron nitride ultrathin film on zinc-blende gallium nitride

J. Pak, W. Lin, K. Wang, A. Chinchore, M. Shi, D. C. Ingram, and A. R. Smith[a)]
Department of Physics and Astronomy, Nanoscale and Quantum Phenomena Institute, Ohio University, Athens, Ohio 45701

K. Sun
Department of Materials Science and Engineering, University of Michigan, Ann Arbor, Michigan 48109

J. M. Lucy, A. J. Hauser, and F. Y. Yang
Department of Physics, The Ohio State University, 191 Woodruff Avenue, Columbus, Ohio 43210

(Received 3 February 2010; accepted 12 April 2010; published 16 June 2010)

The authors report the growth of iron nitride on zinc-blende gallium nitride using molecular beam epitaxy. First, zinc-blende GaN is grown on a magnesium oxide substrate having (001) orientation; second, an ultrathin layer of FeN is grown on top of the GaN layer. *In situ* reflection high-energy electron diffraction is used to monitor the surface during growth, and a well-defined epitaxial relationship is observed. Cross-sectional transmission electron microscopy is used to reveal the epitaxial continuity at the gallium nitride-iron nitride interface. Surface morphology of the iron nitride, similar to yet different from that of the GaN substrate, can be described as plateau valley. The FeN chemical stoichiometry is probed using both bulk and surface sensitive methods, and the magnetic properties of the sample are revealed. © *2010 American Vacuum Society.*
[DOI: 10.1116/1.3425805]

I. INTRODUCTION

Iron nitrides are attractive for their high magnetic moments,[1] corrosion and oxidation resistance,[2] and many other attractive properties. There are various complex phases of iron nitride (Fe_xN_y) such as $Fe_{16}N_2$, Fe_8N, Fe_4N, Fe_3N_2, Fe_2N, and FeN, and the more Fe-rich phases are expected, and have been found, to be magnetic. Motivated by the potential attractive properties, there has been much recent work to explore the Fe-rich Fe_xN_y films using various growth methods including sputtering,[3] nitriding,[4,5] ion implantation,[6] molecular beam epitaxy (MBE),[7,8] and chemical vapor deposition.[9]

Thin film growth of iron nitride having 1:1 stoichiometry has not been well studied, although two 1:1 phases have been proposed—rocksalt (RS-FeN) and zinc-blende (ZB-FeN) phases—with lattice constants of 4.57 and 4.33 Å, respectively.[10,11] There have also been some interesting reports of magnetism in ZB-FeN. A theoretical paper has shown the existence of metastable magnetic states in ZB-FeN for unit cell volumes larger than the equilibrium value.[12] Houari *et al.*[13] reported that the equilibrium energies of nonmagnetic and ferromagnetic states of ZB-FeN are very close, which may be a reason for the micromagnetic character reported experimentally by Suzuki *et al.*[14] It is therefore important to explore the structural and magnetic properties of ZB-FeN grown by MBE.

In previous studies, Fe_xN_y films have been grown on a wide range of conventional cubic structure substrates, such as MgO,[15] GaAs,[16] InGaAs,[17] NaCl,[6] and Ge.[18] Still, a very attractive substrate for FeN growth is zinc-blende gallium nitride (ZB-GaN). Growth of ZB-FeN on ZB-GaN would offer the possibility to form an isocrystalline and isoanion bilayer system with potential electronic or spintronic applications.

One challenge is simply the growth of single-phase FeN films.[19] We previously reported growth of (111)-oriented FeN on wurtzite GaN(0001).[20] In this work, we investigate the growth of FeN on ZB-GaN(001) in an ultrahigh vacuum MBE chamber. We investigate the crystallinity, lattice parameter, and epitaxial quality of the grown layer, as well as the chemical stoichiometry and magnetic properties.

II. EXPERIMENT

The experiments are performed in a custom-designed ultrahigh vacuum MBE system with base pressure of low 10^{-10} Torr. Iron nitride and GaN films are grown using an Fe e-beam evaporator, a Ga effusion cell, and a radio-frequency (rf) nitrogen (N_2) plasma source. The Fe and Ga fluxes are calibrated using a quartz crystal thickness monitor. The N flux is set by the N_2 flow rate and plasma source power.

The substrate for FeN growth is ZB-GaN grown on rocksalt magnesium oxide (MgO) (001). The MgO substrate is first cleaned with acetone and isopropanol, then loaded into the MBE chamber and heated up to 1000 °C for 30 min under nitrogen plasma. The ZB-GaN with (001) orientation is grown at ~750 °C, and then annealed at ~880 °C for 40 min to achieve a 4× reconstructed surface. Details regarding MBE growth of ZB-GaN(001) on MgO(001) have been reported previously.[21,22]

During growth, reflection high-energy electron diffraction (RHEED) using 20 keV electron energy is used to monitor the surface structure and the *in-plane* lattice parameter. After taking the sample out of the chamber, atomic force micros-

a)Electronic mail: smitha2@ohio.edu

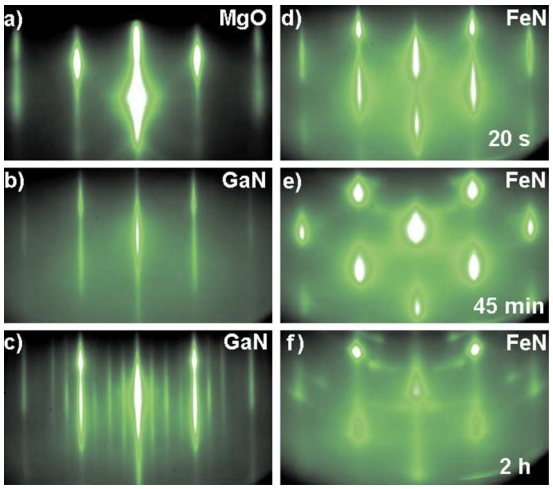

FIG. 1. (Color online) Sequential RHEED patterns for FeN film growth process on ZB-GaN(0 0 1) substrate grown on MgO(0 0 1) substrate, along ⟨110⟩. (a) MgO surface after heating at 1000 °C for 30 min; (b) ZB-GaN surface after growth; (c) ZB-GaN surface after annealing, showing 4× reconstruction; [(d) and (e)] FeN surface during growth; and (f) FeN surface after growth.

copy (AFM) is used to determine the surface morphology, and cross-sectional transmission electron microscopy (XTEM) operating at 300.0 keV is used to assess the interface quality. Rutherford backscattering spectroscopy (RBS) using 2.2 MeV He ions with a backscattering angle of 168° is used to check thickness and bulk chemical stoichiometry. Additionally, energy-dispersive x-ray spectroscopy (EDX), and Auger electron spectroscopy (AES) operated in pulse-counting mode are applied to verify the bulk and surface chemical composition. Finally, the magnetic property is investigated using a superconducting quantum interference device (SQUID) system.

III. RESULTS AND DISCUSSION

A. Growth and in-plane lattice constant evolution

For the FeN film growth reported here, the substrate temperature was set to ~210 °C, the Fe flux to ~2.5 $\times 10^{13}/\mathrm{cm}^2$ s, and the growth chamber pressure to ~9.0 $\times 10^{-6}$ Torr with the rf N plasma forward power set to 500 W. For the growth conditions reported here, the rate of FeN growth was 1.4 ML/min based on the Fe flux rate measured. The total growth time was about 2 h, giving a final expected FeN film thickness of ~360 Å. Later, it is shown from XTEM measurements that the actual FeN film thicknesses are less than expected by ~17%; therefore, in the following discussion, the deposited thicknesses have been corrected by a factor of 0.83. For example, the corrected FeN growth rate is ~1.17 ML/min.

Shown in Fig. 1(a) is the RHEED pattern of a MgO(001) substrate surface along ⟨110⟩ taken before the start of ZB-GaN growth. The streaky pattern indicates a smooth starting substrate surface. Shown in Fig. 1(b) is the RHEED pattern of ZB-GaN taken after the growth at 750 °C. The pattern shows that the growth orientation of the ZB-GaN film conforms to that of the MgO substrate. Shown in Fig. 1(c) is the RHEED pattern taken after annealing the ZB-GaN layer to 880 °C and after cooling to 210 °C. The annealing process results in a semiconducting GaN starting surface for FeN growth which is 4× reconstructed with a tetrahedral-type bonding structure.[21]

Shown in Fig. 1(d) is the RHEED pattern taken 20 s after the start of FeN growth, corresponding to ~1/3 monolayer (ML) of FeN. The 4× reconstruction pattern of ZB-GaN has completely disappeared upon opening the Fe shutter, and the FeN growth shows only a 1× pattern. Since the RHEED pattern maintains the same symmetry for primary (first-order) streaks as the GaN substrate, an epitaxial relationship is found. The in-plane orientation relationship is FeN[100]‖GaN[100] and FeN[110]‖GaN[110]. Consequently, the *out-of-plane* relationship is FeN[001]‖GaN[001].

A fairly streaky pattern is maintained up to about 13 min of deposition, corresponding to ~15 ML. Figure 1(e) is taken at 45 min corresponding to ~53 ML, and we see that a spotty fcc pattern has developed; while the crystallinity is maintained to this point, the FeN layer is no longer as smooth. Figure 1(f) shows at the end of a 2 h growth corresponding to about 140 ML FeN. The RHEED pattern is spotty and also ring patterns have developed, indicating formation of other orientations. Therefore, for best crystalline quality, it is suggested to limit the thickness to smaller values.

If we consider the evolution of lattice constants beginning from the zinc-blende GaN substrate [Fig. 1(c)], we find that there is no change at 1/3 ML [Fig. 1(d)], corresponding to $a \sim 4.52$ Å. In fact, very little change in the lattice constant is observed all the way to 53 ML FeN [Fig. 1(e)], suggesting that the FeN layer is under in-plane tensile stress. However, by 140 ML FeN growth [Fig. 1(f)], the first-order spots give an $a=4.32$ Å, much closer to the bulk zinc-blende FeN value ($a=4.33$ Å) reported in previous papers.[11]

B. Film crystallinity and epitaxial continuity

Cross-sectional high-resolution TEM shows clear evidence for the crystallinity and epitaxial growth of the FeN layer, as shown in Fig. 2. Figure 2(a) shows the large-scale view including MgO substrate, GaN layer, and FeN layer. The interface between GaN and MgO is very obvious; the interface between the FeN and the GaN is also visible as the FeN region has a mottled appearance compared to the GaN layer. By placing markers, we get the FeN layer thickness of ~300 Å and the GaN layer thickness of 3000 Å.

Zooming in, Fig. 2(b) shows the atomic lattice image in the vicinity of the interface between the FeN and GaN layers. No obvious distinction between the two layers can be detected at this scale [note that the line drawn corresponds to the expected location of the interface as determined from large-scale images such as Fig. 2(a) where the interface is visible]. The image of the interface region shows a continuous atomic lattice, corresponding to the fcc sublattice projected onto the (010) plane. A high quality epitaxial growth is

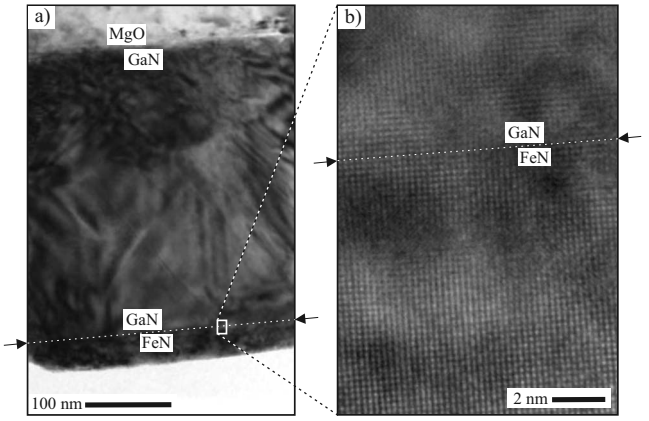

FIG. 2. (a) Large-scale cross-sectional TEM image of an FeN film grown on ZB-GaN; arrow markers indicate the interface between FeN and GaN layers. (b) Zoom-in atomic lattice cross-sectional TEM image in the vicinity of the FeN/GaN interface; arrow markers indicate the expected location of the interface.

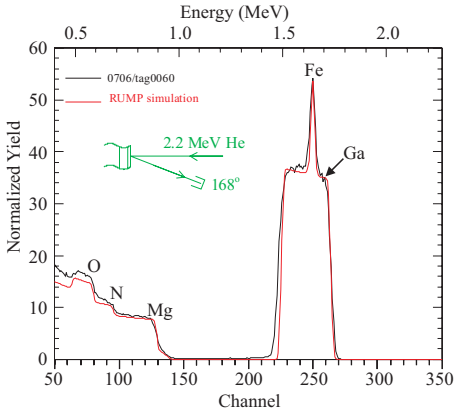

FIG. 4. (Color online) RBS data and RUMP simulation for the FeN/ZB-GaN sample. The Fe peak is located at 1.65 MeV and is on top of the Ga plateau coming from the ZB-GaN substrate layer. The N edge (from FeN and GaN) starts at approximately 0.7 MeV.

apparent. It strongly indicates that the FeN continues with the same crystal structure (zinc blende) as the cubic GaN substrate. The growth is therefore heteroepitaxial, with the FeN lattice being under tensile strain near the interface.

C. Film morphology

Figure 3 shows AFM images of two samples—GaN/MgO [Fig. 3(a)] and FeN/GaN/MgO [Fig. 3(c)]. The image size is 3×3 μm^2. Line profiles for these images are also depicted in Figs. 3(b) and 3(d), respectively. The GaN/MgO film image [Fig. 3(a)] shows a morphology consisting of smooth plateaus, which are separated by some thin but deep crevices. The plateaus have a rather irregular shape. The line profiles show wide plateaus of up to ~3000 Å width with smoothness at the level of 5–10 Å (seen in the close-up line sections) but crevices up to 1000 Å depth (full-width line sections). Since the surface smoothness has previously been observed using scanning tunneling microscopy (STM) to be atomically smooth on the plateau regions,[22] the zoom-in AFM line section is clearly limited by the noise level of the instrument. Overall, the image is consistent with large GaN islands, which merged to form a continuous film.

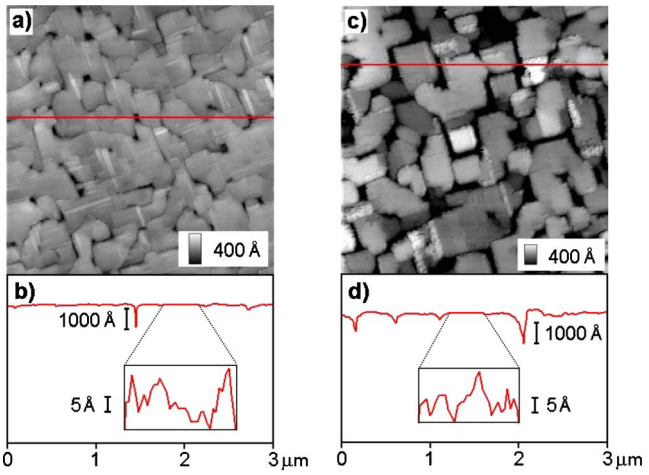

FIG. 3. (Color online) AFM images and line profile measurements of ZB-GaN and FeN films. (a) AFM image of ZB-GaN after annealing, (b) line profile measurements of ZB-GaN film, (c) AFM image of FeN film grown for 2 h on ZB-GaN, and (d) line profile measurements of FeN film. The insets in (b) and (d) show zoom-ins of plateau regions indicating 5–10 Å smoothness.

Considering the AFM image of the FeN/GaN/MgO film [Fig. 3(c)], we see a very similar morphology consisting of smooth plateaus separated by deep crevices. The line profiles again show wide plateaus with 5–10 Å smoothness and crevices up to 1000 Å depth. Furthermore, root-mean-square roughness analysis on the plateau regions shows that the FeN and GaN film surfaces have similar values (18 Å for GaN versus 17 Å for FeN/GaN), and again these values are certainly limited by the AFM noise level. From the RHEED pattern [Fig. 1(f)], the FeN film definitely has a more three-dimensional character compared to the GaN surface.

Also seen in both images are some thin-line-like features, which run along orthogonal crystallographic directions. The origin of these features is as-of-yet unknown, but in any case they are seen in both the GaN and FeN/GaN samples.

One obvious distinct difference in the two images is that on a larger scale, for the FeN/GaN film, the plateau regions appear to have receded away from each other as compared to the plateau regions of the GaN film, which are fairly well directly adjacent to each other. For example, although both images are displayed with a similar gray scale, the FeN/GaN image has much more valley areas (dark areas) in between the plateau areas. This difference could be interpreted as evidence of a transition to a more three-dimensional (3D) growth mode for the FeN film compared to the two-dimensional (2D) GaN growth mode.

D. Chemical content

In this section three independent investigations of the chemical content of the FeN/GaN layers are presented. First, in Fig. 4, a second sample grown under similar conditions

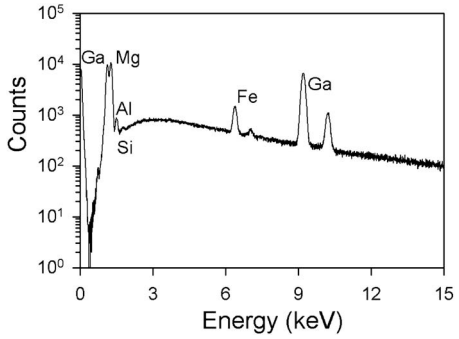

FIG. 5. EDX data showing the existence of Fe and Ga in the sample. Some other peaks, including Si and Al, are attributed to impurities residing within the MgO substrate.

(but different thicknesses) was examined using RBS. The Fe peak is seen superimposed on top of the Ga plateau and is quite narrow due to the very thin FeN layer. The RBS data (random spectrum) were simulated using the RUMP code[23] with FeN and GaN layers having the equivalent of ~2770 Å GaN and 190 Å FeN. The bulk stoichiometry determined using the RUMP fitting is Fe/N=1.0.

Presented in Fig. 5 are EDX spectra acquired on the FeN/GaN sample. Similar to RBS, EDX spectroscopy is sensitive to the elemental composition of the bulk of the thin film sample. As can clearly be seen, both Fe and Ga peaks are clearly present, confirming the existence of both Fe- and Ga-containing layers. The N peak is not seen in the EDX spectrum due to its energy being below the energy cutoff of the system. The Fe and Ga peaks are seen all across the uniform film surface area.

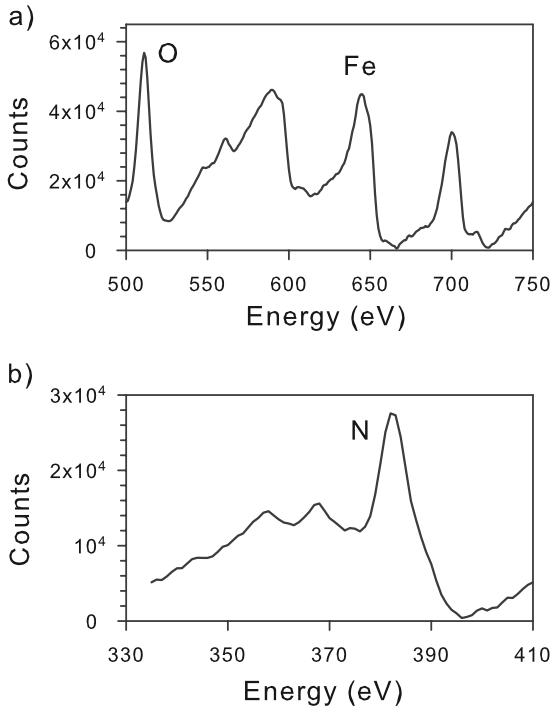

FIG. 6. Plots of AES pulse-counting (not derivative) data showing existence of Fe and N at the surface. No peaks were found in the Ga spectral region (not shown here).

To probe the chemical content of the FeN layer surface, we apply AES to an FeN/ZB-GaN sample, as shown in Fig. 6. AES is sensitive to the elemental composition of the top few surface atomic layers of the sample. Figures 6(a) and 6(b) show the clear existence of Fe and N (respectively) at the atomic surface of the sample. Importantly, no Ga peaks were seen in the AES spectrum, indicating that Ga has not diffused to the FeN surface. Calculation of the derivative peak-peak amplitude values for the 705 eV Fe peak (P_{Fe}) and 389 eV N peak (P_N), combined with tabulated relative sensitivity factors $S_{Fe}=0.9168$ and $S_N=0.9157$, relevant for a 5 keV primary electron beam, allows a quantitative Fe/N surface ratio estimation using the equation[24]

$$\mathrm{Fe/N} = \frac{P_{Fe}/S_{Fe}}{P_N/S_N}. \quad (1)$$

This analysis results in a ratio of 1.2. After a further calibration correction has been applied, we get an Fe/N ratio of approximately 0.9, indicating the possibility of a slightly N-rich surface but consistent with the RBS bulk measurement within 10% uncertainty.

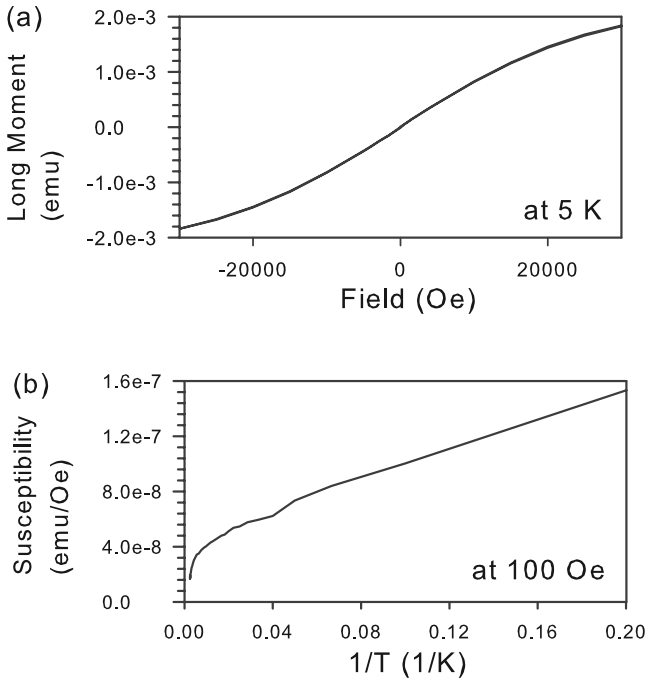

FIG. 7. SQUID measurement of FeN/ZB-GaN(001) film. (a) magnetization vs field, and (b) susceptibility vs $1/T$.

E. Magnetic properties

To determine the magnetic properties of the FeN film, we have applied SQUID magnetometry. The results are presented in Fig. 7. As can be seen in Fig. 7(a), the magnetization versus applied field acquired at 5 K shows no evidence of ferromagnetism; rather, the data show a monotonic in-

crease in magnitude of the moment with increase in magnitude of the field (with a linear region at low field magnitude), and there is no evidence of any hysteresis. This behavior is paramagnetic.

The paramagnetism is further confirmed by the temperature dependence of the susceptibility, as shown in Fig. 7(b), which was acquired at an applied field of 100 Oe. The linear variation with $1/T$ is consistent with Curie's law for paramagnetism. The paramagnetic result proves that the film is neither elemental Fe (with strong magnetic moment) nor an Fe-rich Fe_xN_y phase such as Fe_4N.

This result may be compared to theoretical expectations. According to Houari *et al.*,[13] the zinc-blende phase should be nonmagnetic, whereas the rocksalt phase should be ferromagnetic. This further confirms that our sample must be in the zinc-blende phase. The fact that the sample was grown on a zinc-blende template may be the reason.

IV. CONCLUSIONS

It has been shown in this article that FeN(001) ultrathin films can be heteroepitaxially grown on ZB-GaN(001)/MgO(001) substrates with good crystallinity as revealed by RHEED and XTEM. The epitaxial orientation is determined to be FeN[110]∥GaN[110] and FeN[100]∥GaN[100]. Based on the orientation relationship, measured in-plane lattice parameter, and epitaxial continuity, the crystal structure of the FeN is concluded to be zinc blende. Up to at least 50 ML, the FeN film is found to be strained with tensile in-plane strain. The FeN epitaxial quality over the strained region appears to be good as indicated by XTEM, while the AFM analysis reveals a distinct change to a more 3D growth as compared to the GaN sample, which shows 2D growth, and this is consistent with the RHEED results.

Chemical analysis by means of RBS, EDX, and AES results in the conclusion that the MBE-grown FeN layer has a stoichiometry of $Fe/N=0.9-1.0$ with no evidence for Ga in the surface layer. Magnetic measurements presented here show that the sample is paramagnetic. Plans for further studies of the growth of Fe_xN_y films having larger Fe:N compositions and thus ferromagnetic properties on GaN substrates are in progress.

ACKNOWLEDGMENTS

This study is supported by the Department of Energy, Office of Basic Energy Sciences (Grant No. DE-FG02-06ER46317). Additional support from the National Science Foundation (Grant No. 0730257) is also acknowledged.

[1]T. K. Kim and M. Takahashi, Appl. Phys. Lett. **20**, 492 (1972).
[2]S. F. Matar, G. Demazeau, and B. Siberchicot, IEEE Trans. Magn. **26**, 60 (1990).
[3]S. R. Kappaganthu and Y. Sun, Surf. Coat. Technol. **167**, 165 (2003).
[4]K. H. Jack, J. Alloys Compd. **222**, 160 (1995).
[5]M. Wohlschlogel, U. Welzel, and E. J. Mittemeijer, Appl. Phys. Lett. **91**, 141901 (2007).
[6]E. Leroy, C. Djega-Mariadassou, H. Bernas, O. Kaitasov, R. Krishnan, and M. Tessier, Appl. Phys. Lett. **67**, 560 (1995).
[7]D. M. Borsa, S. Grachev, D. O. Boerma, and J. W. J. Kerssemakers, Appl. Phys. Lett. **79**, 994 (2001).
[8]H. Takahashi, M. Igarashi, A. Sakuma, and Y. Sugita, IEEE Trans. Magn. **36**, 2921 (2000).
[9]J. Zheng, R. Yang, W. M. Chen, L. Xie, X. G. Li, and C. P. Chen, J. Phys. D: Appl. Phys. **42**, 185209 (2009).
[10]H. Nakagawa, S. Nasu, H. Fujii, M. Takahashi, and F. Kanamaru, Hyperfine Interact. **69**, 455 (1992).
[11]T. Hinomura and S. Nasu, Physica B **237–238**, 557 (1997).
[12]Y. Kong, J. Phys.: Condens. Matter **12**, 4161 (2000).
[13]A. Houari, S. F. Matar, M. A. Belkhir, and M. Nakhl, Phys. Rev. B **75**, 064420 (2007).
[14]K. Suzuki, H. Morita, T. Kaneko, H. Yoshida, and H. Fujimori, J. Alloys Compd. **201**, 11 (1993).
[15]M. Takahashi, H. Shoji, H. Takahashi, H. Nashi, T. Wakiyama, M. Doi, and M. Matsui, J. Appl. Phys. **76**, 6642 (1994).
[16]M. Komuro, Y. Kozono, M. Hanazono, and Y. Sugita, J. Appl. Phys. **67**, 5126 (1990).
[17]Y. Sugita, H. Takahashi, M. Komuro, K. Mitsuoka, and A. Sakuma, J. Appl. Phys. **76**, 6637 (1994).
[18]X. Ding, F. Zhang, J. Yan, H. Shen, X. Wang, X. Liu, and D. Shen, J. Appl. Phys. **82**, 5154 (1997).
[19]L. Rissanen, M. Neubauer, K. P. Lieb, and P. Schaaf, J. Alloys Compd. **274**, 74 (1998).
[20]W. Lin, J. Pak, D. C. Ingram, and A. R. Smith, J. Alloys Compd. **463**, 257 (2008).
[21]H. A. AL-Brithen, R. Yang, M. B. Haider, C. Constantin, E. Lu, A. R. Smith, N. Sandler, and P. Ordejon, Phys. Rev. Lett. **95**, 146102 (2005).
[22]M. B. Haider, R. Yang, C. Constantin, E. Lu, A. R. Smith, and H. A. H. Al-Brithen, J. Appl. Phys. **100**, 083516 (2006).
[23]L. R. Doolittle, Nucl. Instrum. Methods Phys. Res. B **9**, 344 (1985).
[24]*Handbook of Auger Electron Spectroscopy*, 3rd ed. (Physical Electronics, Inc., Eden Prairie, MN, 1995), p. 17.